PHILOSOPHICAL TRANSACTIONS OF THE ROYAL SOCIETY A
MATHEMATICAL, PHYSICAL & ENGINEERING SCIENCES

Metal and Phosphide Phases in Luna 24 Soil Fragments

H. J. Axon, M. J. Nasir and F. Knowles

Phil. Trans. R. Soc. Lond. A 1980 **297**, 7-13
doi: 10.1098/rsta.1980.0199

METAL AND PHOSPHIDE PHASES IN LUNA 24 SOIL FRAGMENTS

By H. J. AXON, M. J. NASIR and F. KNOWLES
Metallurgy Department, Grosvenor Street, The University, Manchester M1 7HS, U.K.

(*Communicated by G. Eglinton, F.R.S. – Received* 21 *February* 1979)

[Plates 1 and 2]

CONTENTS

Soil fragments in the 106–150 and 150–250 μm size ranges were selected for metallographic and microprobe examination on the basis of their magnetic properties. Serial sections of the mounted fragments were examined. One fragment proved to be a compositionally zoned crystal of phosphide with no metal phase but partly embedded in glass. Another was a coarse-grained association of silica with ilmenite and fayalite with a 5 μm particle of metallic iron in troilite. One splinter of oxide contained a central spine of metallic iron. The remaining six fragments contained 10 μm particles of iron–nickel–cobalt alloy with compositions in either the 'meteoritic' or the low Ni – low Co sub-meteoritic composition ranges of Ni, Co content. In some fragments separate particles of alloy had different Ni, Co contents. No particles of high Co metal were encountered.

Previous work

Friel & Goldstein (1977) reported on the metal phases in the U.S. allocation of Luna 24 soil samples. They examined polished thin sections from core levels 24109, 24149, 24170, 24174 and 24210 as part of a consortium study and noted that less than 3% of the soil fragments showed visible metal. They analysed a total of 17 metal particles from 9 polished thin sections and detected no variation of metal composition with stratigraphy. Their two largest pieces of metal both had compositions within the Ni+Co range that is associated with iron meteorites. Their largest piece measured 100 μm × 125 μm and contained inclusions of nickeliferous FeS. Their second largest piece measured 40 μm × 60 μm, was compositionally zoned and also contained inclusions of nickeliferous FeS. However, most of the particles analysed by Friel & Goldstein were in the form of *ca.* 10 μm bodies in glass–breccia agglutinates and had Ni + Co compositions in the range from pure iron up to about 4.6% Ni, 0.5% Co. In addition they encountered three particles of high cobalt content, namely 8.2Ni, 0.97Co; 37.2Ni, 1.58Co, 26.8Ni, 2.39Co. The sizes of these particles are not reported.

Present work

The present investigation was conducted on a total of eleven fragments of soil in the size ranges 106–150 and 150–250 μm selected on the basis of their magnetic properties from Luna 24 soil at levels 24090, 24125 and 24196. The fragments were selected by Dr Pillinger and Mrs Fabian (see previous paper) and were supplied in small glass capsules. The fragments were mounted in cold-setting metallurgical mounting compound and were polished by conventional metallographic methods with the aim of producing on each fragment a number of serial sections at approximately 15 μm intervals. Previous studies of the metal in this type of lunar soil fragment have relied upon a single arbitrary section plane. The metal was studied by optical metallography and was analysed for Ni and Co with the use of conventional microprobe procedures with metallic standards and correction programs similar to the work reported from this laboratory by Axon & Nasir (1977) and Sears & Axon (1976*a*). Further analytical investigation was conducted on some of the particles by using the scanning electron microscope with solid-state analytical facilities according to the 'standardless' method of analysis developed by Nasir (1976). In this method the X-ray spectrum emitted by a multi-element specimen and detected by an energy dispersive solid state device is apportioned to the mass percentages of the individual elements observed in the specimen. In principle this is done by using theoretical models of X-ray generation to normalize the X-ray intensity generated within the specimen by each element. This is further corrected for absorption and fluorescence effects in the system. Tables of correction factors have been presented by Nasir (1976) and have been extended to cover all the necessary K, L and M lines for voltages in the range 15–40 kV for most elements of the periodic table.

As in the work of Friel & Goldstein (1977), most of the metallic particles were in the size range about 10 μm. Smaller particles were not usually analysed. The few larger particles are discussed in the text.

Results

Analyses of metal particles

In table 1 the results of the conventional microprobe investigation are recorded, in terms of mass percentages Ni or Co, for the metal according to the stratigraphic level and size range of each soil fragment. Table 1 also records our laboratory designation L1, etc., the corresponding microphotograph, the serial section when metal was encountered in more than one section, and also the silicate–metal association. It will be remembered that Friel & Goldstein's (1977) observations were made on polished thin sections. Consequently they were able to characterize the silicate type in some detail. However, the serial sectioning approach of the present work allowed observation in reflected light only. Consequently the silicate–metal associations in table 1 are reported according to the scheme of Goldstein *et al.* (1972).

Table 1. Microprobe analyses of Luna 24 metal and phosphide particles

soil fragment		analysis (% by mass) Ni	Co	metal–silicate association†			
24090							
106–150	L1	0.1	n.d.	II 1 (I) FeS	see table 2		figures 5, 6, 7
106–150	L2	n.a.	n.a.	I 2–3	α_2 distorted metal		figure 11
106–150	L3	10.2	n.d.	exotic	16.6 % Cr stainless steel		
150–250	L11	2.8	0.2	II 1 (0)	—		figure 10
		1.8	0.4	0	—		
24125							
106–150	L4	2.2	0.4	II 1 (0)	average-full square		figure 1
106–150	L6	0.4	0.0	II oxide	splinter of metal in oxide circle in figure 1		
150–250	L10	2.1	0.3	II 2–3 (I)	—		
106–150	L5	11.6	0.36	II 2–3	phosphide, 15.9 % P		figure 2
		10.1	n.a.	globules		serial section 1	figure 2
		11.5	0.33	II 2–3	at edge	serial section 2	
		16.7	0.40		at centre	serial section 2	
		n.a.	n.a.	0		serial section 3	
		—	—	0	figure 4	serial section 4	figure 3
24196							
106–150	L7	0.4	0.1	II 2–3 (0)	—	serial section 1	
		2.2	0.4	II 2–3 (0)	—	serial section 2	
		1.4	0.4	II 2–3 (I)	vein	serial section 2	
		1.2	0.3	II 2–3 (I)	vein full triangle in figure 1	serial section 3	figure 9
106–150	L8	5.9	0.4	II 2–3 (0)		serial section 1	
		7.4	0.6	II 2–3 (0)	larger metal	serial section 2	figure 8
		7.8	0.5	II 2–3 (0)	—	serial section 4	
150–250	L12	1.8	0.3	II 1 (0)			

n.d., not detected; n.a., not analysed.

† Key to metal–silicate associations as visible in each plane of section: 0, metal or metallic phase with no attached silicate; I 2–3, major metal, peripheral breccia + glass; II 1 (0), major crystalline silicate, minor metal at periphery; II 1 (I), major crystalline sulphide, minor metal inside sulphide; II 2–3 (0), major breccia + glass, minor peripheral metal; II 2–3 (I), major breccia + glass, minor interior metal.

In table 1, particle L3 is a flake-like piece of metal measuring 120 μm × 40 μm with no associated oxide or silicate. It contains no cobalt but has 10.2 % Ni and 16.6 % Cr. It has a mechanically deformed appearance and could be a fragment of swarf from a stainless steel. It is labelled exotic in table 1. Goldstein *et al.* (1972) recorded the presence of a similar fragment (no. 22.6) but with 17 % Cr, 81 % Fe in their Apollo 14 soil sample.

Particle L5 is a massive crystal of phosphide without associated metal. It is discussed in detail in the next section.

Particle L6 is a thin splinter, of length about 200 μm. It contains a central spine of iron with 0.37 % Ni surrounded by magnetite with an outer layer of goethite. So far as the authors are aware, no identical material has been reported from lunar soils.

Particle L1 is a minute, *ca.* 5 μm, crystal of essentially pure iron, associated with a small, *ca.* 10 μm, area of troilite within a very coarsely crystalline mass of silica, ilmenite and fayalite. Details of the s.e.m. 'standardless' analysis of the non-metallic phases in this particle are given in the next section.

The remainder of the particles in table 1 are similar to the populations reported by Friel

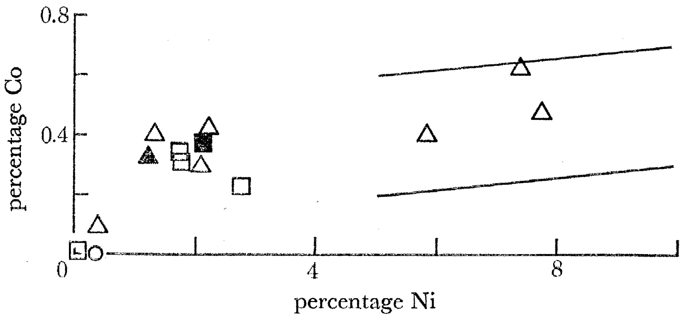

FIGURE 1. Ni and Co analyses for metal particles in Luna 24 soil fragments. Most particles of metal were in the 10 μm size range. Symbols indicate silicate association; squares represent metal in crystalline rock; triangles represent metal in breccia or glass. The circle represents the metal-oxide fragment L6. The lines indicate the field of 'meteoritic' composition.

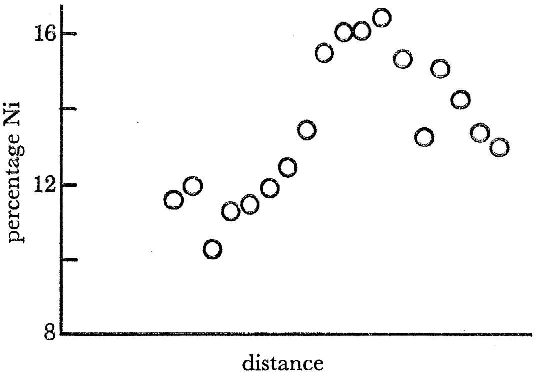

FIGURE 4. Variation of nickel content with distance across the line shown in figure 3 for the compositionally zoned phosphide, soil fragment L5, serial section 4. The smooth variation of nickel content is disturbed by cracking in the phosphide crystal.

& Goldstein at low Ni, low Co compositions and at compositions within the meteoritic range. However, no instance of high Co material was encountered in the present work. The compositions are plotted in figure 1, from which it may be seen that of a total of 14 analytical observations, 3 lie within the so-called 'meteoritic' composition range while 11 lie within the low Ni, low Co range. This situation may be compared with the findings of Friel & Goldstein who, from a total of 17 analytical points, found 2 in the 'meteoritic' range, 12 in the low alloy range and 3 in the high Co range.

In the present work the larger fragments of soil appeared in general to be less well endowed with metal. In most cases the metal tended to lie in the size range 10–15 μm and it was fairly common for a single soil fragment to act as host to more than one particle of metal. Thus, the four metal particles analysed in specimen L4 show essentially the same composition and their values may be reasonably averaged, but in other instances particles of metal of different composition were encountered in the same soil fragment. This is especially true of fragments L7 and L8, both of which come from the 24196 level of the core sample. Single sections from these fragments are shown in figure 8† (L8, the largest of the meteoritic particles – at serial section 2) and in figure 9 (the vein of non-meteoritic composition at serial section 3 of L7).

† Figures 2, 3, 5–7 appear on plate 1 and figures 8–11 on plate 2.

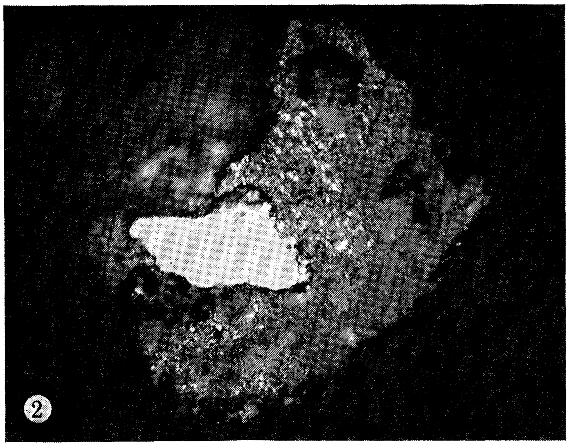

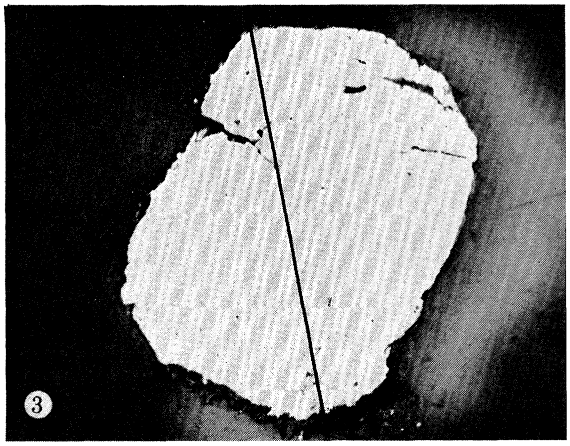

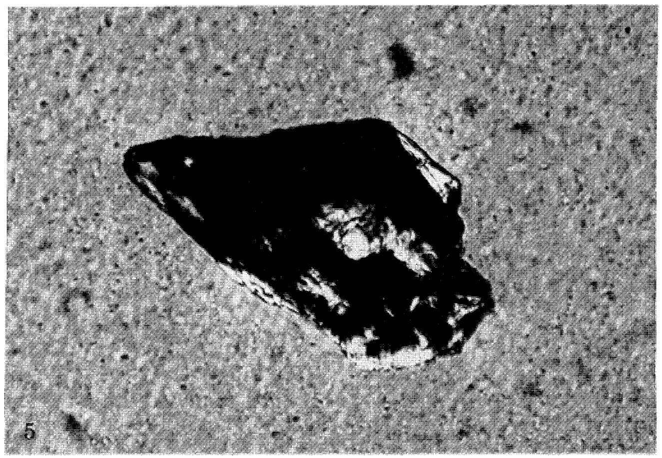

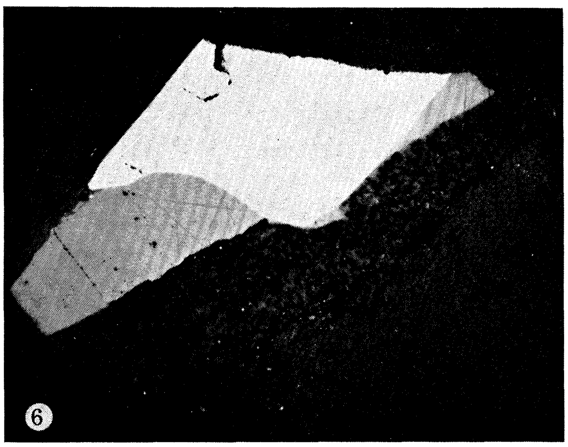

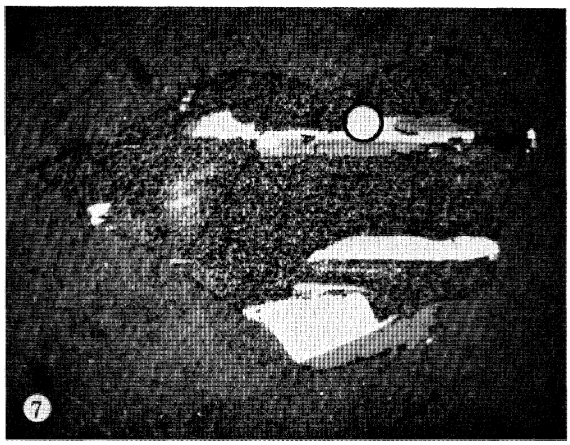

FIGURE 2. Serial section 1 of fragment L5 showing a compositionally zoned phosphide 50 μm × 20 μm partly encased by glass and breccia. The glass contains a multitude of phosphide globules. Reflected light. Unetched.

FIGURE 3. Serial section 4 of the phosphide particle shown in figure 2. The phosphide now shows the development of crystal faces and is free of silicate associations. Microprobe analyses of the Ni content across the marked diameter are shown in figure 4. The length of the probe trace is 110 μm. Reflected light. Unetched.

FIGURE 5. Transmitted light photograph of fragment L1 mounted in metallurgical mounting agent. The angular fragment measures 150 μm × 260 μm and consists of very coarse opaque crystals in an optically transparent (silica) matrix.

FIGURE 6. Serial section 2 of fragment L1, showing ilmenite, bright, fayalite, smooth grey, and silica, rough, dark. Analyses in table 2. No metal in this section. Reflected light, unetched. Field of view 150 μm × 190 μm.

FIGURE 7. Serial section 4 of fragment L1, showing ilmenite, fayalite and silica. A small association of metal + troilite was encountered in the area indicated. Analyses in table 2. Reflected light, unetched. Field of view 190 μm × 240 μm.

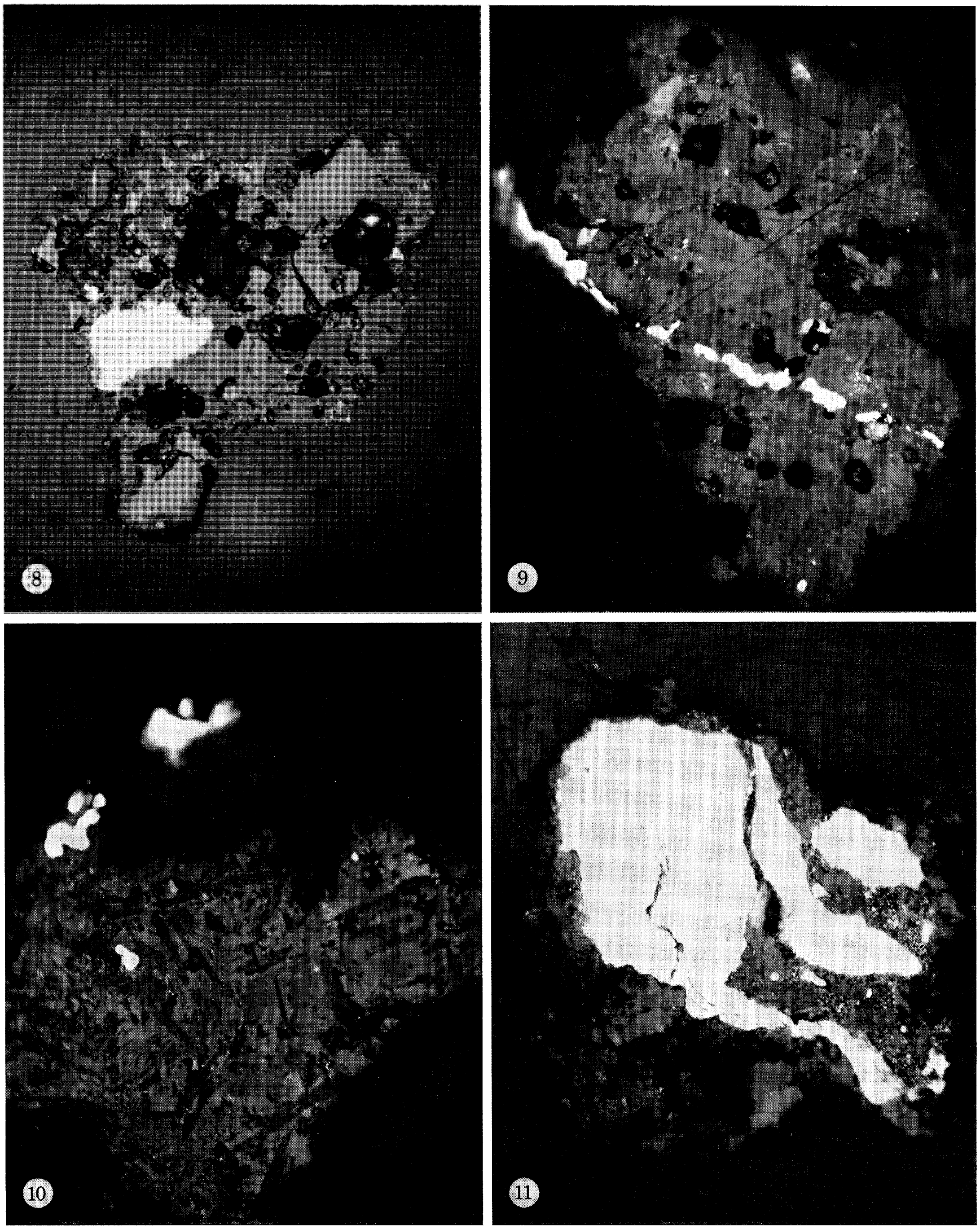

FIGURE 8. Serial section 2 of fragment L8 showing the larger particle of metal of 'meteoritic' composition 7.4 % Ni, 0.6 % Co. The other two particles of metal in this fragment are similar in size and location to the particles in figure 10 but are of 'meteoritic' composition. Reflected light. Unetched. Field of view 150 μm × 190 μm.

FIGURE 9. Serial section 3 of fragment L7 showing a vein of metal of average composition 1.2 % Ni, 0.3 % Co. Metal of at least two other 'submeteoritic' compositions is encountered in other sections of this fragment. Reflected light. Unetched. Field of view 150 μm × 190 μm.

FIGURE 10. Fragment L11 showing three particles of metal. One small particle totally embedded in the crystalline silicate not analysed. The triple particle at the edge of the silicate has 2.8 % Ni, 0.2 % Co. The larger and apparently free-standing particle beyond the edge of the silicate has 1.8 % Ni, 0.4 % Co. Reflected light. Unetched. Field of view 150 μm × 190 μm.

FIGURE 11. Fragment L2 showing a large distorted fragment of metal with glass and breccia associations. This particle on etching shows a polycrystalline structure of distorted kamacite. Similar particles have been encountered in the 'sub-meteoritic' composition range of Apollo soil. Reflected light. Unetched. Field of view 130 μm × 170 μm.

The non-metallic particles

Soil fragment L5 from the 24125 level proved to be a phosphide particle of considerable size without any associated metal phases. Serial sectioning revealed that the particle was free-standing for much of its length and in its free-standing region it showed the suggestion of crystallographically developed faces (figure 3). However, as shown by the earlier serial sections, one end of the phosphide crystal was associated with a dispersion of minute phosphide globules within a glassy host (figure 2). The data reported in table 1 indicate that the phosphide contained 15.9% P, about 0.35% Co and was compositionally zoned with respect to nickel. The Ni variation across a diameter of the section of crystal shown in figure 3 is plotted in figure 4 and shows that the Ni content decreases from about 16.5% at the centre to about 11.5% at the edge. It is noteworthy that the Ni content in the early sections tends to be low and that of the globules embedded within the glassy material of the early sections tends to be even lower. The value of 10.1% Ni reported in table 1 for the globules of serial section 1 is an average of 9.32, 9.13, 12.27, 10.27, 7.85, 10.77, 9.68 and 11.35 measured on eight of the larger globules. These observations are consistent with the idea that an idiomorphic, free-standing crystal of compositionally zoned phosphide became splashed with glass so that some of the phosphide was incorporated as globules in the glass. The absence of metallic phases and the direction of compositional zoning are unusual and suggest that the phosphide may have grown from the vapour phase rather than within a metallic host. From the available evidence, it is not possible to be more specific about the history of this phosphide.

Previous detailed studies of phosphides in Apollo lunar soils have been concerned with relatively small particles of phosphide in association with a metallic phase. The compositions at these metal–phosphide interfaces have enabled Axon & Goldstein (1972) to estimate equilibration temperatures by reference to the known Fe–Ni–P equilibrium diagrams. Unfortunately, in that work the Co content of the phosphide was not usually measured. However, values for metal–phosphide associations were obtained in two instances of Apollo 17 soil 78501, namely a γ+phosphide association of metal containing 32.0% Ni, 1.55% Co and less than 0.02% P, with phosphide containing 49.9% Ni, 0.51% Co and 15.5% P, and an α+phosphide association in which the corresponding values were 2.5, 0.75, 0.09 and 13.9, 0.11, 15.5. In each case the Co tends to be higher in the metal than in the phosphide. The distribution of Co between the α and phosphide phases in the (less cobaltic) iron meteorites has not been extensively studied but preliminary studies in this laboratory on the Tocopilla hexahedrite indicate more than 0.4% Co in the α phase as against less than 0.15% Co in the phosphide.

Soil fragment L1 is unusual among metal-containing lunar soil particles in that it is a coarse-grained mixture of opaque and transparent material (figure 5). Early sections (figure 6) showed neither metal nor sulphide and examination in the s.e.m. with the use of the solid state detection facility for analysis and the 'standardless' method of Nasir (1976) showed that the transparent material was SiO_2 and the opaque phases were ilmenite and fayalite. Later sections (figure 7) again showed a matrix of SiO_2 with opaque inclusions of ilmenite, fayalite and other mineral phases but with one minute area of troilite and metallic iron. A selection of analyses obtained by the 'standardless' method, but with a stoichiometric distribution of oxygen sufficient to convert the metals to their appropriate oxides, is given in table 2. This soil fragment may be interpreted as coarse mesostasis material consisting of silica, fayalite and ilmenite with a minor amount of troilite and metallic iron.

Table 2. 'Standardless' analyses of non-metallic phases in fragment L1

	fayalite	ilmenite	troilite
SiO_2	34.93	—	—
TiO_2	—	52.8	—
FeO	58.77	47.4	—
MnO	0.63	—	—
MgO	4.93	—	—
CaO	0.74	—	—
Fe	—	—	62.52
S	—	—	37.47

Discussion

Most of the soil fragments examined in the present work have structures and metal compositions similar to those previously encountered in other lunar returned samples, although no examples of high Co metal were encountered. The metal that was encountered in the so-called 'meteoritic' composition range and in the low Ni – low Co composition range occurred in relative proportions similar to those reported by Friel & Goldstein (1977) at different levels in the Luna 24 core. It is, of course, important to recognize that the so-called 'meteoritic' composition range on the Ni–Co plot represents the experimentally determined *bulk* compositions of the majority of iron meteorites that have fallen on Earth in relatively recent times. The bulk composition of the metal in many chondrites appears to fall in this range also. However, Sears & Axon (1976*b*) have shown that the metal in LL chondrites may be considerably enriched in both Ni and Co and thus occupy positions above the meteoritic band. Moreover, while the meteoritic composition band for the irons is based on bulk compositions, M. J. Nasir (unpublished results) has shown that in the vicinity of coarse phosphide bodies the relative distribution of Ni and Co between the phosphide and metal phases may produce within the iron meteorite local areas of metal that are depleted in Ni and enriched in Co. These areas are bounded by laths of brittle phosphide and are of a size appropriate to the small volumes of metal encountered in lunar soils. Thus, for small particles of metal there can be no absolute correspondence between Ni–Co composition in the 'meteoritic' range and meteoritic origin.

Nevertheless, it has been widely assumed that the Moon has been subjected to bombardment by meteoritic projectiles of composition similar to that of present-day iron meteorites and the sub-meteoritic low Ni – low Co metals that compose most of the grains analysed both by Friel & Goldstein (1977) and in the present work may be reasonably interpreted as diluted meteoritic material.

All three examples of metal compositions in the 'meteoritic' range were encountered in the single fragment L8. We were unable to detect any certain difference between the mode of occurrence of 'meteoritic' and 'submeteoritic' compositions in our range of material, except that one of the 'meteoritic' particles was unusually large (figure 8) (L8 serial section 2). However, the other 'meteoritic' particles in L8 were similar in size and shape to the 'sub-meteoritic' particles illustrated in figures 9 and 10.

No analysis was obtained for particle L2 (figure 11), and no serial sections are available because this particle was lost in processing. However, on etching with 1 % Nital the metal showed single-phase microcrystalline, distorted kamacite and had an appearance and association similar to the heavily deformed particles of α reported in Apollo 14 by Goldstein *et al.* at 4.0% Ni, 0.4% Co (particle 27.14 with breccia) and at 3.7% Ni, 0.3% Co (particle 26.14 with glass).

The serial sectioning procedure proved useful in the present work from two points of view. First, it allowed us to find and examine the metal in those fragments of soil that were not heavily endowed. Such fragments do not necessarily show metal on a single arbitrary section. Secondly, it revealed the three-dimensional distribution and composition variations when larger quantities of metal (or phosphide) were present. The study of the phosphide particle (figures 2 and 3) is one of the most interesting cases, but the development of the vein-like distribution of metal in L7 (figure 9) is also very informative. The small externally located particles of metal in sections 1 and 2 of this fragment have greatly different compositions, 0.4–2.2% Ni; also in section 2 a string of metal particles appears in vein-like form extending from the edge of the silicate to approximately the centre and shows a third composition at 1.3% Ni. This appears, by its orientation, to develop into the completely transecting vein of metal that is shown in figure 9. In addition it will be seen from table 1 that the three metal analyses in the 'meteoritic' range arose from sections 1, 2 and 4 of the same fragment of soil and it is most unlikely that these different metals would have been revealed by any single arbitrary section.

References

Axon, H. J. & Goldstein, J. I. 1972 *Earth planet. Sci. Lett.* **16**, 439–447.
Axon, H. J. & Nasir, M. J. 1977 *Mineralog. Mag.* **41**, 121–122.
Friel, J. J. & Goldstein, J. I. 1977 *Geophys. Res. Lett.* **4**, 481–483.
Goldstein, J. I., Axon, H. J. & Yen, C. F. 1972 In *Proc. III Lunar Sci. Conf.* (Suppl. 3, *Geochim. cosmochim. Acta*), vol. 1, pp. 1037–1064. M.I.T. Press.
Nasir, M. J. 1976 *J. Microsc.* **108**, 79–87.
Sears, D. W. & Axon, H. J. 1976*a* *Nature, Lond.* **260**, 34–35.
Sears, D. W. & Axon, H. J. 1976*b* *Meteoritics* **11**, 97–100.

PHILOSOPHICAL TRANSACTIONS OF THE ROYAL SOCIETY A MATHEMATICAL, PHYSICAL & ENGINEERING SCIENCES

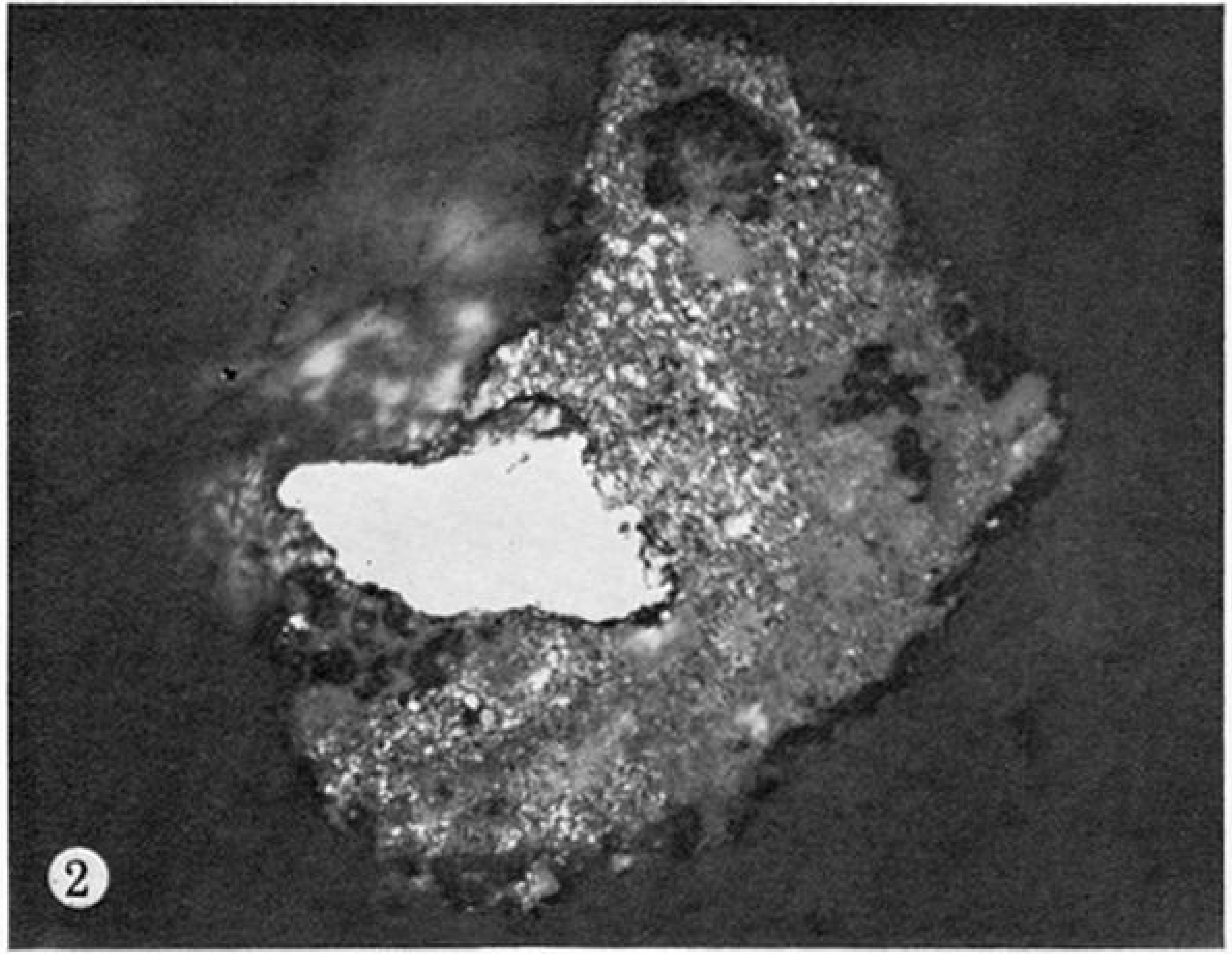

FIGURE 2. Serial section 1 of fragment L5 showing a compositionally zoned phosphide 50 μm × 20 μm partly encased by glass and breccia. The glass contains a multitude of phosphide globules. Reflected light. Unetched.

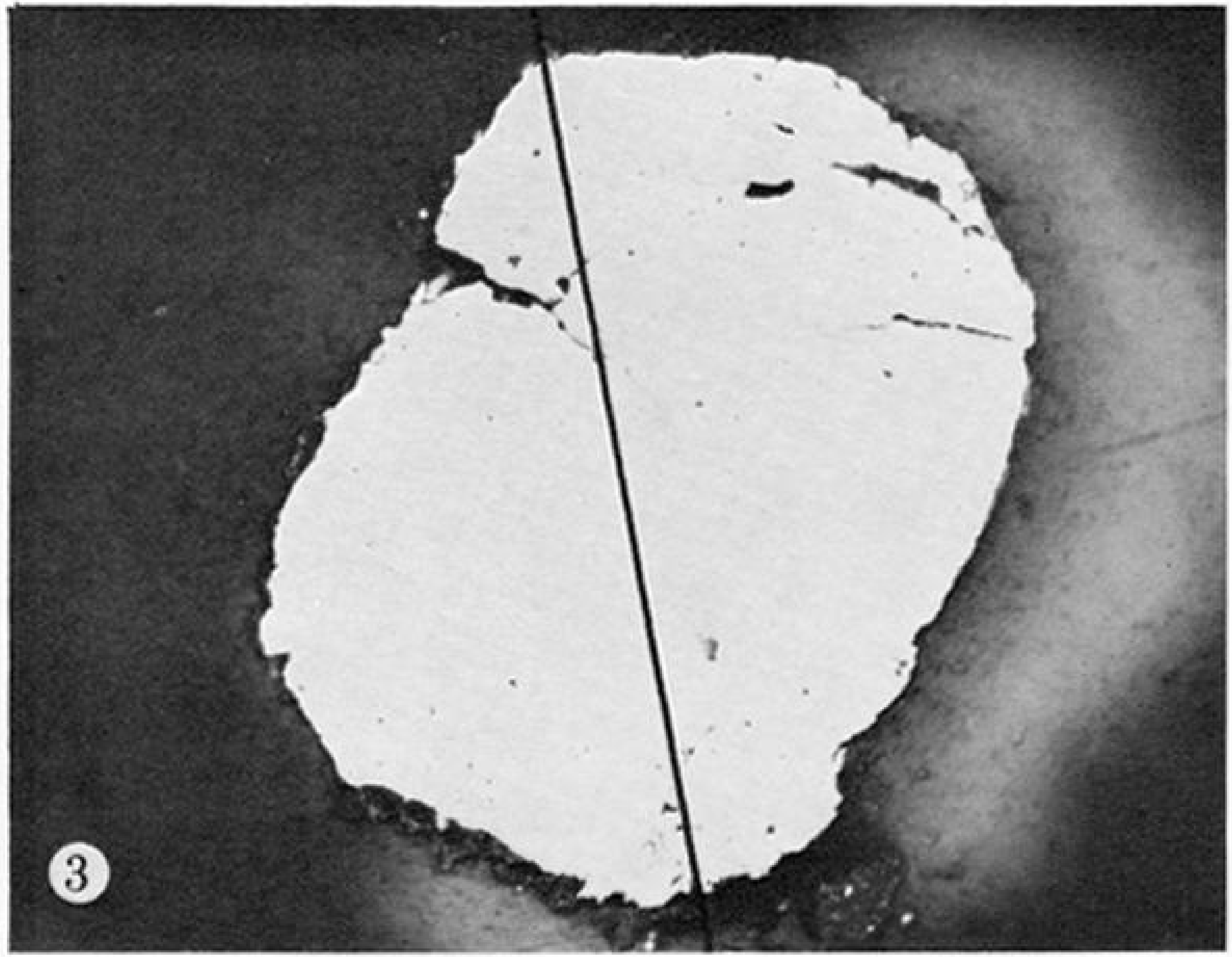

FIGURE 3. Serial section 4 of the phosphide particle shown in figure 2. The phosphide now shows the development of crystal faces and is free of silicate associations. Microprobe analyses of the Ni content across the marked diameter are shown in figure 4. The length of the probe trace is 110 μm. Reflected light. Unetched.

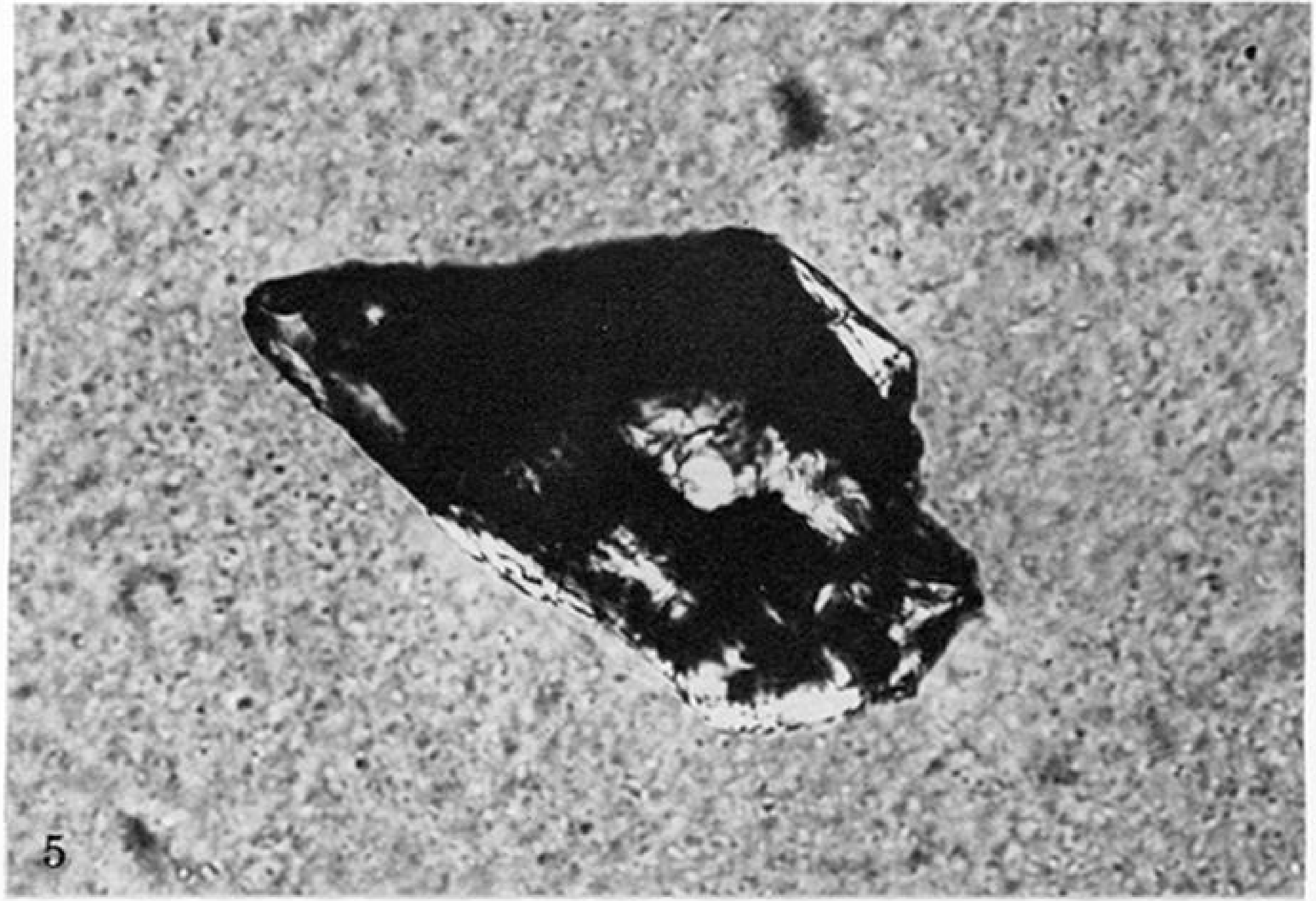

FIGURE 5. Transmitted light photograph of fragment L1 mounted in metallurgical mounting agent. The angular fragment measures 150 μm × 260 μm and consists of very coarse opaque crystals in an optically transparent (silica) matrix.

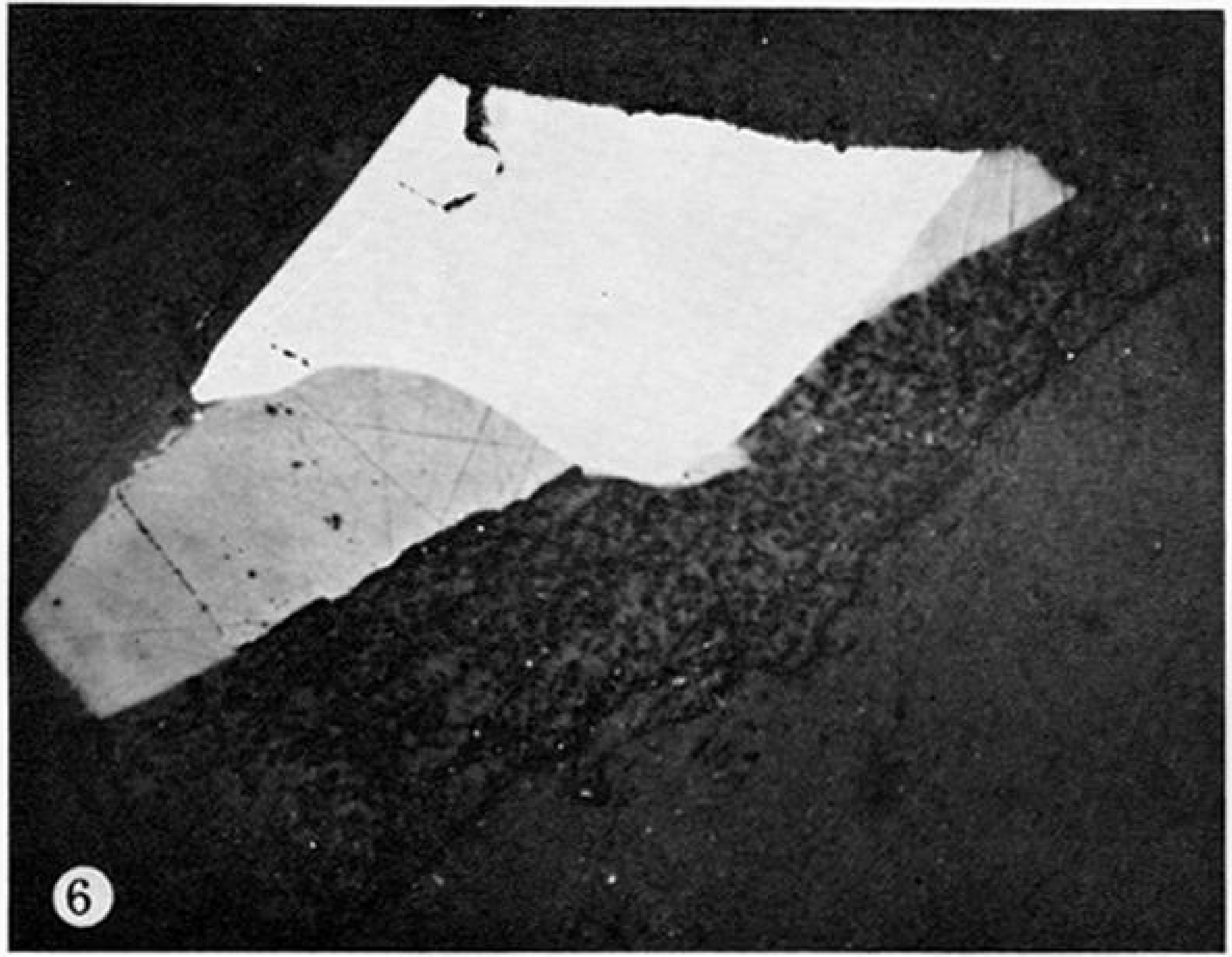

IGURE 6. Serial section 2 of fragment L1, showing ilmenite, bright, fayalite, smooth grey, and silica, rough, dark. Analyses in table 2. No metal in this section. Reflected light, unetched. Field of view 150 µm × 190 µm.

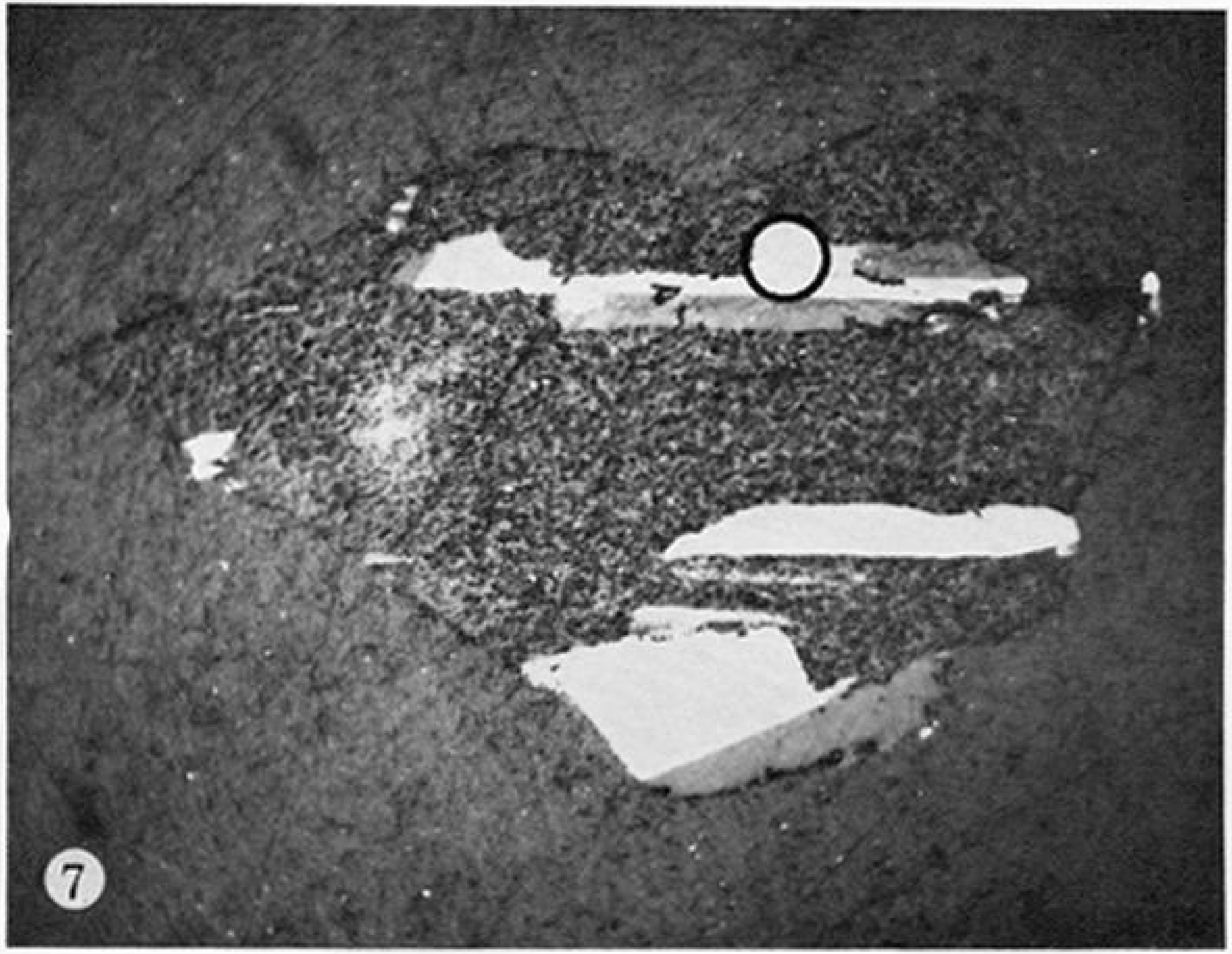

FIGURE 7. Serial section 4 of fragment L1, showing ilmenite, fayalite and silica. A small association of metal + troilite was encountered in the area indicated. Analyses in table 2. Reflected light, unetched. Field of view 190 μm × 240 μm.

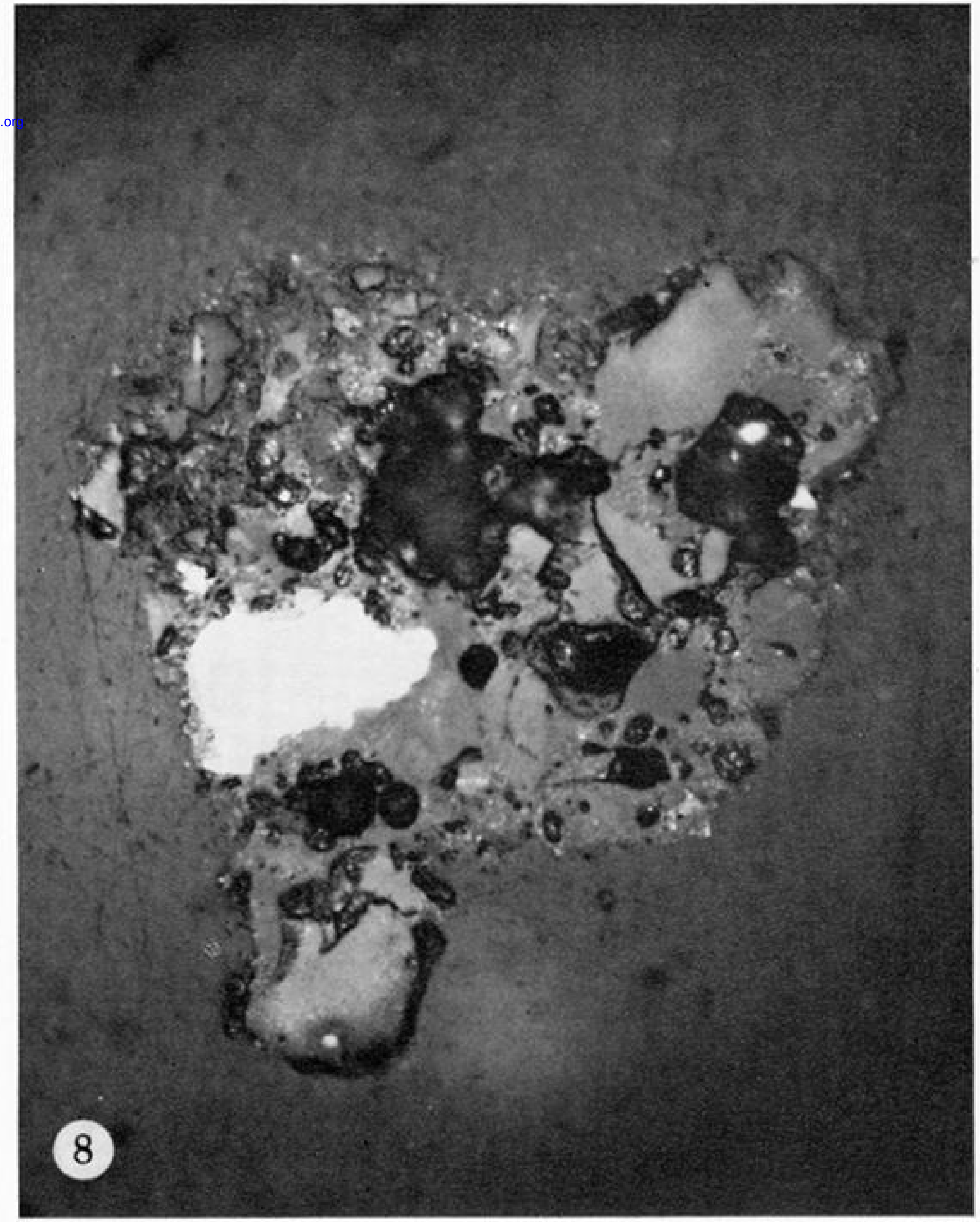

IGURE 8. Serial section 2 of fragment L8 showing the larger particle of metal of 'meteoritic' composition 7.4 % Ni, 0.6 % Co. The other two particles of metal in this fragment are similar in size and location to the particles in figure 10 but are of 'meteoritic' composition. Reflected light. Unetched. Field of view 150 μm × 190 μm.

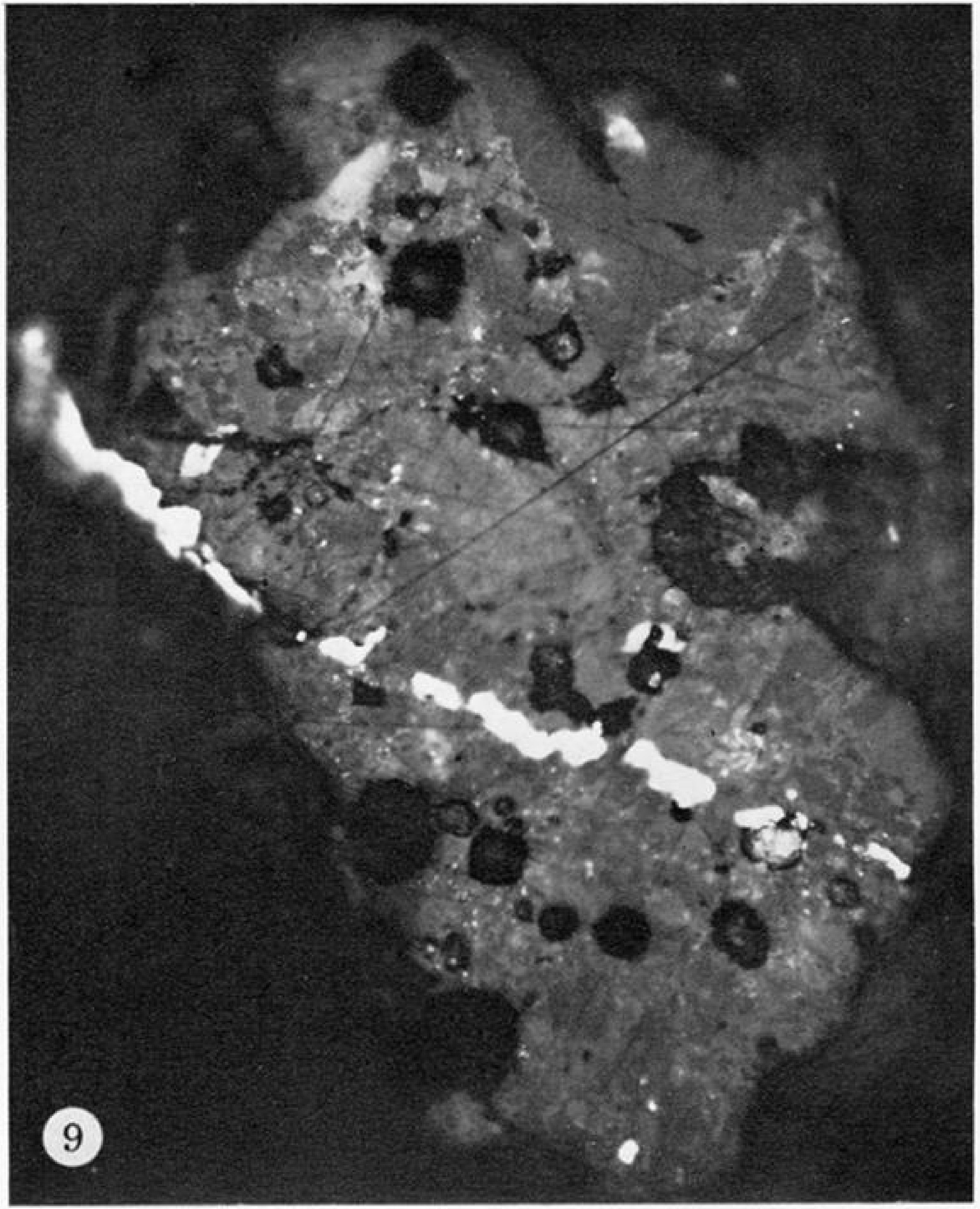

FIGURE 9. Serial section 3 of fragment L7 showing a vein of metal of average composition 1.2 % Ni, 0.3 % Co. Metal of at least two other 'submeteoritic' compositions is encountered in other sections of this fragment. Reflected light. Unetched. Field of view 150 μm × 190 μm.

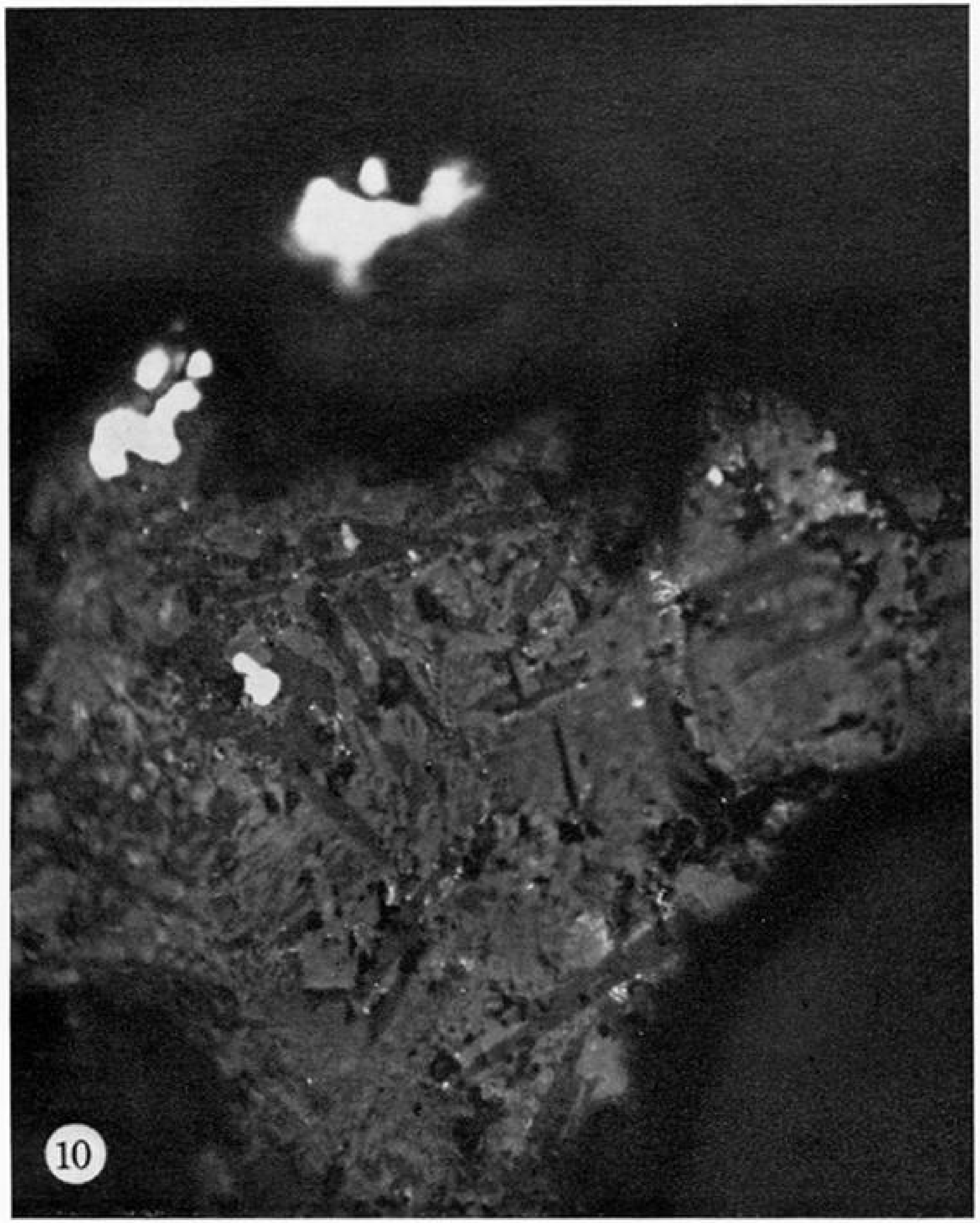

FIGURE 10. Fragment L11 showing three particles of metal. One small particle totally embedded in the crystalline silicate not analysed. The triple particle at the edge of the silicate has 2.8 % Ni, 0.2 % Co. The larger and apparently free-standing particle beyond the edge of the silicate has 1.8 % Ni, 0.4 % Co. Reflected light. Unetched. Field of view 150 μm × 190 μm.

PHILOSOPHICAL TRANSACTIONS OF THE ROYAL SOCIETY A MATHEMATICAL, PHYSICAL & ENGINEERING SCIENCES

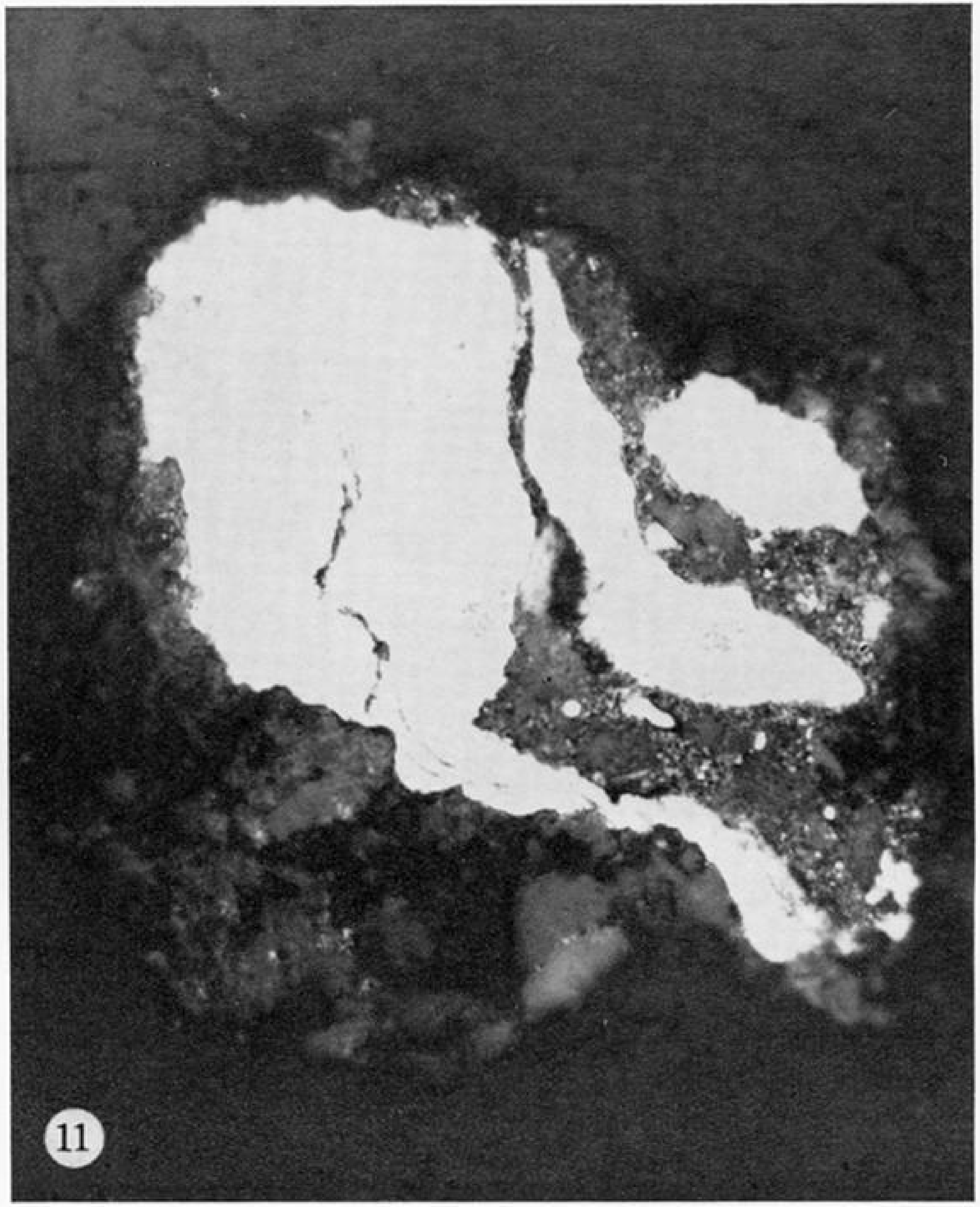

FIGURE 11. Fragment L2 showing a large distorted fragment of metal with glass and breccia associations. This particle on etching shows a polycrystalline structure of distorted kamacite. Similar particles have been encountered in the 'sub-meteoritic' composition range of Apollo soil. Reflected light. Unetched. Field of view 130 μm × 170 μm.

PHILOSOPHICAL TRANSACTIONS OF THE ROYAL SOCIETY A MATHEMATICAL, PHYSICAL & ENGINEERING SCIENCES